

FUZZY CONTROLLER AND PWM INVERTER FOR CONVEYOR BELT SYNCHRONIZATION

Dan Alexandru STOICHESCU, Dumitru STANCIU

"Politehnica" University of Bucharest, Electronics and Telecommunications Faculty
Bd. Armata Poporului, 1-3, Sect. 6, Bucharest, Romania
Fax +401 410 3921 E-mail: stoich@vl.elia.pub.ro

ABSTRACT

In the paper, a fuzzy controller and a PWM inverter for conveyor belt synchronization are presented. The fuzzy controller corrects the speed of the belt transporting the packing boxes in order to synchronize the meeting of the products with their corresponding packing boxes. A control method of a single phase inverter resulting in a load frequency twice the inverter switching frequency is described.

Keywords: fuzzy controller, membership functions, PWM inverter.

1. INTRODUCTION

The system is made up of two conveyor belts A and B, used for products packing. The belt A, transporting the products, shifts with constant speed and the belt B transporting the packing boxes shifts with variable speed. The belts are moved by special d.c. electric motors.

The belt B may be accelerated or decelerated so that the moment of the meeting of the belt A product with the belt B box will correspond to the desired packing up moment. The system has sensors able to measure the distance "x" between the product and its box and the time variation " $\Delta x/\Delta t$ " of this distance, too. The belt B speed is modified depending on the distance "x" and its time variation $\Delta x/\Delta t$, by the fuzzy controller.

2. DESCRIPTION OF THE BLOCK DIAGRAM

The block diagram of the B band speed control power electronic circuit which realizes the synchronization between the product and the corresponding packing is shown in **fig. 1**.

The fuzzy controller (1) corrects the d.c. motor speed " Δv " and in the same time B band speed in terms of the distance "x" and its derivative $\Delta x/\Delta t$.

The speed reference value ($v^* + \Delta v$) and the real motor speed (v_m) are algebraically added, the speed control being realized by the PI speed controller (2). The current is limited particularly during the motor start by the PI regulator (3); its output and the speed regulator (2) output are connected to the positive minimum gate (4). The output of this gate and the bipolar triangular wave generator (6) output are connected to the comparator (5). The comparator outputs are connected to the gates of the IGBT type transistors T1-T4, through specialized optoelectronic circuits (7) providing electrical insulation.

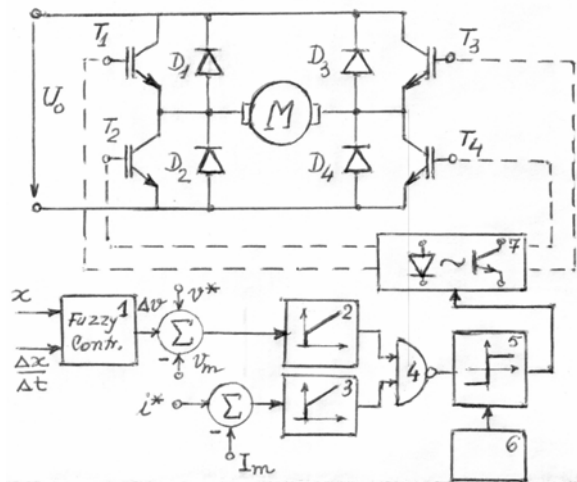


Fig. 1. Block diagram of the power electronic system

3. THE FUZZY CONTROLLER

In [2], [3], [6] and [7], a.c. motor speed adjusting fuzzy controllers are described; mostly they are using the torque direct control; in [4] fuzzy controllers for d.c. motor speed and current adjustment are presented.

Further, a d.c. motor speed adjusting fuzzy controller is described; it controls a conveyor band, synchronizing the meeting of the product with its packing box.

The fuzzy controller design steps are the following: fuzzification, set of rules, inference, defuzzification.

3.1. Fuzzification. The inputs of the fuzzy controller are the distance "x" between the product and its packing and the derivative $\Delta x/\Delta t$; its output is the speed correction signal Δv of the conveyor belt B.

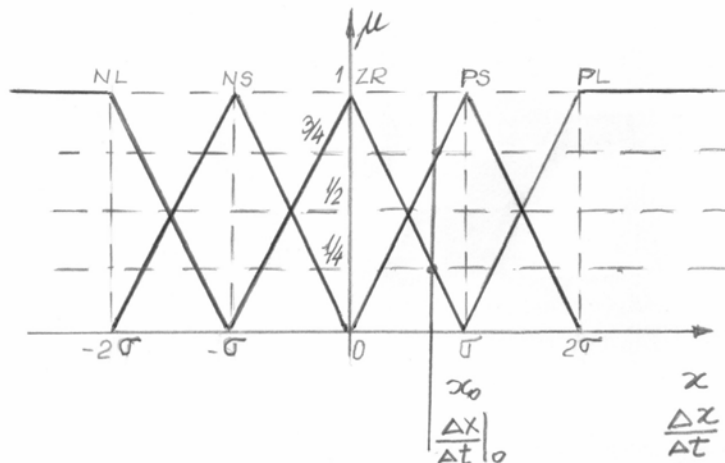


Fig. 2. The membership function for distance x (mm) and variation $\Delta x/\Delta t$ (mm/s)

The membership classes used for the distance "x" as well as for " $\Delta x/\Delta t$ " are the same, that is: NL, NS, ZR, PS and PL; for the output " Δv ", the membership classes are: NL, NM, NS, ZR, PS, PM, PL.

The membership functions for "x" and for $\Delta x/\Delta t$ are shown in **fig. 2**, and the membership function of the output signal " Δv " is shown in **fig. 3**.

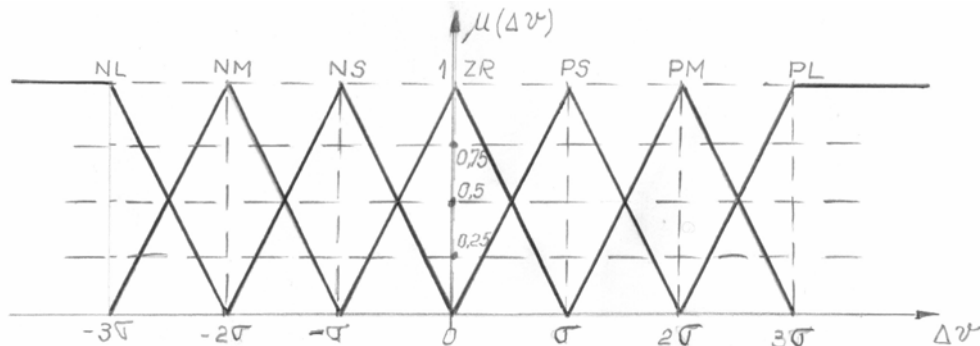


Fig. 3. The membership function for speed Δv (mm/s)

The triangular membership degrees shown in **fig. 2** and **3** are generated by the function

$$\mu = y - [y] \quad (1)$$

where $[y]$ is the integer of y .

In **fig. 2**: $y = \pm x / \sigma + 2 \quad (2)$

For input "x", $\sigma = 25\text{mm/s}$ and for input $\Delta x / \Delta t$, $\sigma = 10\text{mm/s}$

In **fig. 3**: $y = \pm x / \sigma + 3 \quad (3)$

For output " Δv ", $\sigma = 6,6\text{mm/s}$

3.2. The set of rules. As the controller has two inputs and one output, the rules may be matricially expressed. These rules are sentences of the following type:

If $x = ?$ and $\Delta x / \Delta t = ?$, then $\Delta v = ?$

The rules matrix is shown in **fig. 4**.

$\begin{matrix} x \\ \Delta x \\ \Delta t \end{matrix}$	NL	NS	ZR	PS	PL
NL	NM	NS	PS	PM	PL
NS	NM	NS	PS	PM	PL
ZR	NM	NS	ZR	PS	PM
PS	NL	NM	NS	PS	PM
PL	NL	NM	NS	PS	PM

Fig. 4. The rules matrix

3.3. Inference. For inference, the MAX-PROD criterion has been used. For the inputs having the values in **fig. 2**, only the gray coloured rules are valid (applicable).

The membership degree of every active rule is determined using the product in the following way:

$$m_1 = \mu_{ZR}(x_0) \cdot \mu_{ZR}(\Delta x/\Delta t|_0) = 1/4 \cdot 1/4 = 1/16$$

$$m_2 = \mu_{ZR}(x_0) \cdot \mu_{PS}(\Delta x/\Delta t|_0) = 1/4 \cdot 3/4 = 3/16$$

$$m_3 = \mu_{PS}(x_0) \cdot \mu_{ZR}(\Delta x/\Delta t|_0) = 3/4 \cdot 1/4 = 3/16$$

$$m_4 = \mu_{PS}(x_0) \cdot \mu_{PS}(\Delta x/\Delta t|_0) = 3/4 \cdot 3/4 = 9/16$$

The membership degree of every active set of the output signal is determined, also, using the product:

$$\mu_{ZR}^*(\Delta v) = m_1 \cdot \mu_{ZR}(\Delta v) \text{ — a triangular function results having the maximum height.}$$

$$\mu_{ZR}^*(\Delta v)_{\max} = m_1 \cdot \mu_{ZR}(\Delta v)_{\max} = 1/16 \cdot 1 = 1/16$$

Similarly,

$$\mu_{NS}^*(\Delta v) = m_2 \cdot \mu_{NS}(\Delta v) \text{ and } \mu_{NS}^*(\Delta v)_{\max} = m_2 \cdot \mu_{NS}(\Delta v)_{\max} = 3/16$$

For $\mu_{PS}^*(\Delta v)$ two values are resulting:

$$\text{The first value: } \mu_{PS1}^*(\Delta v) = m_3 \cdot \mu_{PS}(\Delta v) \text{ and } \mu_{PS1}^*(\Delta v)_{\max} = m_3 \cdot \mu_{PS}(\Delta v)_{\max} = 3/16$$

$$\text{The second value: } \mu_{PS2}^*(\Delta v) = m_4 \cdot \mu_{PS}(\Delta v) \text{ and } \mu_{PS2}^*(\Delta v)_{\max} = m_4 \cdot \mu_{PS}(\Delta v)_{\max} = 9/16$$

As one can see, for $\mu_{PS}^*(\Delta v)$, two values have been found: $\mu_{PS1}^*(\Delta v)$ and $\mu_{PS2}^*(\Delta v)$.

In order to solve this problem, the "MAX" is applied:

$$\max [\mu_{PS1}^*(\Delta v), \mu_{PS2}^*(\Delta v)] = \mu_{PS2}^*(\Delta v)$$

3.4. Defuzzification. In this case, for defuzzification, the MAX criterion between $\mu_{ZR}^*(\Delta v)$, $\mu_{NS}^*(\Delta v)$ and $\mu_{PS2}^*(\Delta v)$, has to be applied; the hachured surface in **fig. 5** is obtained.

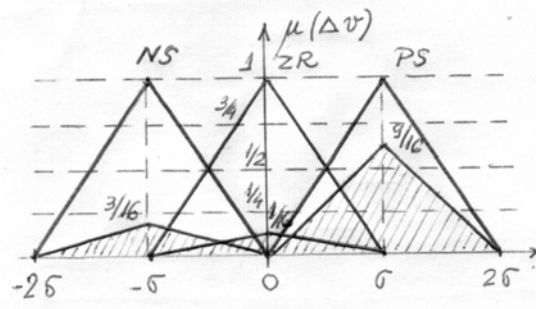


Fig. 5. Defuzzification

For defuzzification we used the formula

$$\Delta v_0 = \frac{\sum \Delta v_i \cdot \mu_i}{\sum \mu_i} \quad (4)$$

– where μ_i is the maximum membership degree (the height) of a hachured triangular function and Δv_i is the corresponding abscissa.

For the case taken into consideration, we get: $\Delta v_0 = 6\sigma/13$

* – As it results from the rules matrix (**fig. 4**), in defuzzification two or three membership classes may be active, so "i" may take the value 2 or 3.

4. PWM CONTROL DOUBLING THE LOAD SWITCHING FREQUENCY

As it results from [6], for the single phase full bridge inverter there are two distinct control modes:

- symmetric control mode: transistors T1 and T4 are switched on simultaneously for a direction of the current, T2 and T3 being off in this interval of time; for the opposite direction of the current, T2 and T3 are on and T1, T4 are off. The same leg transistors T1, T4, respectively T2, T3 are switched in push-pull;
- asymmetric control mode: transistors T3 and T4 are switched on alternatively, every one for a direction of the output current; T1 and T2 are commutated with the switching frequency.

According to fig. 1, the PWM control doubling the load commutation frequency is based on the waveform in **fig. 6**. The PWM control doubling the load switching frequency may be achieved in two ways: a) the generator (6) generates two triangular waves in opposition which are compared to the signal u_R provided by the positive minimum gate (4); b) the generator (6) delivers an unique triangular wave which is compared to u_R and $-u_R$.

The results of these comparisons are the T1...T4 IGBT gate control signals. The load voltage and current are also shown in **fig. 6**.

The load voltage and current waveforms are similar to those resulting in the asymmetric control mode, but their frequency is twice the inverter transistors switching frequency.

If we consider the d.c. motor as a RLE series circuit (where the electromotive voltage E is proportional to the speed), the equivalent diagrams in **fig. 7** are resulting: **fig. 7a** diagram for increasing current and **fig. 7b**, diagram for decreasing current.

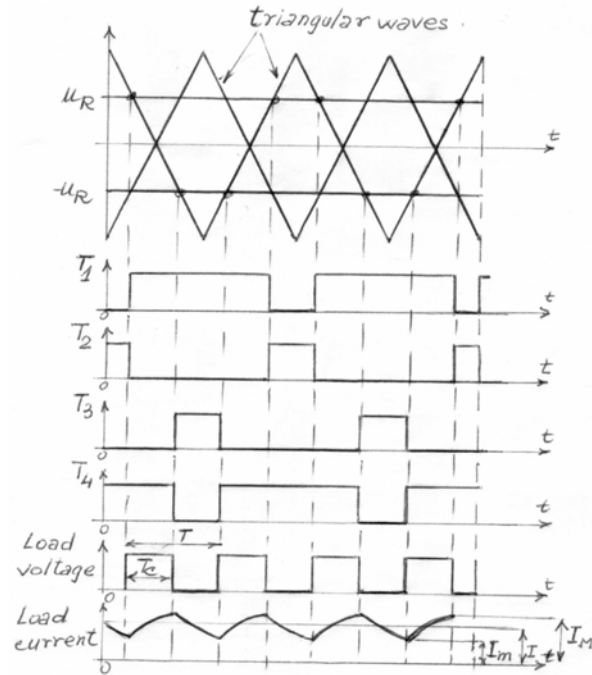


Fig.6. PWM control doubling the load switching frequency

Taking into consideration the waveforms in **fig. 6** and the equivalent circuits in **fig. 7**, the following is resulting:

– For the rising current in the electric circuit of **fig. 7a**, one can write:

$$i_T(t) = (U_0 - E) / R - [(U_0 - E) / R - I_M] e^{-t/\tau} \quad (5)$$

where $\tau = L/R$

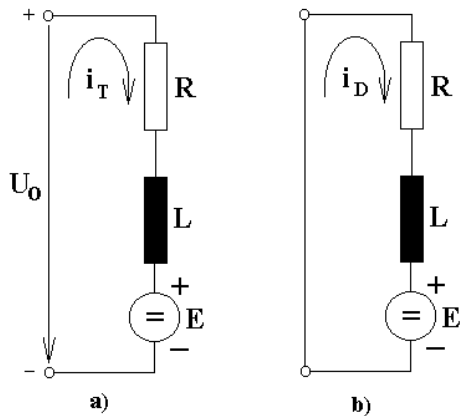


Fig. 7. Equivalent diagrams of inverter:

a) for increasing current

b) for decreasing current

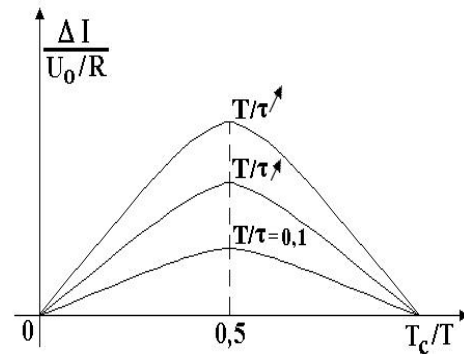


Fig. 8. $\frac{\Delta I}{U_0/R}$ versus T_c/T

– For the decreasing current in the electric circuit of **fig. 7b**, one can write:

$$i_D(t) = -E / R + (E / R + I_M) e^{-(t-T_c)/\tau} \quad (6)$$

At $t = T_c$, $i_T = I_M$ in the expression (5):

$$I_M = (U_0 - E) / R - [(U_0 - E) / R - I_M] e^{-T_c/\tau} \quad (7)$$

At $t = T$, $i_D = I_m$ in the expression (6):

$$I_m = -E/R + (E/R + I_M) e^{-(t-T_c)/\tau} \quad (8)$$

From (7) and (8) the current ripple $\Delta I = (I_M - I_m)/2$ results:

$$\Delta I = \frac{U_0}{R} \frac{1}{\operatorname{cth} \frac{T_c}{2\tau} + \operatorname{cth} \frac{T - T_c}{2\tau}} \quad (9)$$

From (9) it results that the load current ripple ΔI is independent of the load electromotive voltage E .

The graphs $\frac{\Delta I}{U_0/R} = f(T_c/T)$ for different values of T/τ , are shown in **fig. 8**. For a given

value of T/τ , $\frac{\Delta I}{U_0/R}$ is maximum for $T_c/T = 0,5$ and this maximum grows up when T/τ grows up.

The graphs $\frac{\Delta I}{U_0/R} = f(T/\tau)$ for different values of T_c/T are looking almost like a family of parallel lines growing with T/τ and identical for values of T_c/T symmetrical to 0,5.

This control method has been experienced by the authors, waveforms similar to those in **fig. 6** being obtained.

5. CONCLUSIONS

In the paper a speed control power electronic system for synchronizing the product and its packing box belts shifts in a packing equipment is presented.

The fuzzy controller adjusting the packing boxes transporting belt speed in order to synchronize the meeting between a product and its corresponding packing box, is described. The authors contribution to the design of this controller are underlined that is: a triangular membership functions generation method for the input and output signals and a defuzzification method asking much less computing time than the gravity center defuzzification method.

A control method of the single phase inverter resulting in a load frequency twice the inverter switching frequency is also described.

6. REFERENCES

1. BERNADETTE, B. M.; (1993) La logique floue, Presses Universitaires de France
2. HOFMANN, W.; KRAUSE, M.; (1993) Fuzzy control of AC – Drives Fed by PWM Inverters, *Intelligent Motion Conference*, p. 129 – 132
3. MIR, S.; ZINGER, D.; ELBULUK, M.; (1994) Fuzzy Controller for Inverter Fed. Induction Machines, *IEEE Transactions on Industry Applicatins*, vol. 30; nr. 1; p. 78 – 84
4. SOUSA, D.C.; BOSE, K. B.; (1994) A Fuzzy Set Theory Based Control of a Phase – Controlled Converter D.C. Machine Drive, *IEEE Transactions on Industry Applications*, vol. 30; nr. 1, p. 34 – 44
5. GLAZENKO, T.A.; (1971) Amplificatoare de impulsuri cu semiconductoare în acționări electrice, Editura Tehnică
6. BICA, A.; STANCIU, D.; BUȚĂ, V.; (1996) The advantages of Fuzzy Logic Applications to Direct Torque Control Drives, *7th International Power Electronics and Motion Control Conference*, PEMC, Budapest, vol. III, p. 3 453 – 3 456
7. STANCIU, D.; BUȚĂ, V.; BADEA, B.; DINA, B.; (1996) Comparative Study of direct Torque Control Methods, *International Conference on Automation and Quality Control*, A&Q 96, Cluj – Napoca, vol. I, p. 195 – 200